

# Mapping on the HEALPix grid

M. R. Calabretta<sup>1</sup>

Australia Telescope National Facility, PO Box 76, Epping, NSW 1710, Australia

Preprint submitted to astro-ph on 2004/12/23

**Abstract.** The natural spherical projection associated with the Hierarchical Equal Area and isoLatitude Pixelisation, *HEALPix*, is described and shown to be one of an infinite class not previously documented in the cartographic literature. Projection equations are derived for the class in general and it is shown that the HEALPix projection suggests a simple method (a) of storing, and (b) visualising data sampled on the grid of the HEALPix pixelisation, and also suggests an extension of the pixelisation that is better suited for these purposes. Potentially useful properties of other members of the class are described. Finally, the formalism is defined for representing any member of the class in the FITS data format.

**Key words.** astronomical data bases: miscellaneous – cosmic microwave background – cosmology: observations – methods: data analysis, statistical – techniques: image processing

## 1. Introduction

The Hierarchical Equal Area and isoLatitude Pixelisation, *HEALPix* (Górski et al. 2004) offers a scheme for distributing  $12N^2$  ( $N \in \mathbb{N}$ ) points as uniformly as possible over the surface of the unit sphere subject to the constraint that the points lie on a relatively small number ( $4N - 1$ ) of parallels of latitude and are equally spaced in longitude on each of these parallels. These properties were chosen to optimise spherical harmonic analysis and other computations performed on the sphere.

In fact, HEALPix goes further than simply defining a distribution of points; it also specifies the boundary between adjacent points and does so in such a way that each occupies the same area. Thus HEALPix is described as an *equal area pixelisation*. Pixels at the same absolute value of the latitude have the same shape, though pixel shape differs between latitudes. The boundaries for  $N = 1$  define the 12 *base-resolution pixels* and higher-order pixelisations are defined by their regular subdivision. Note, however, that although they are four-sided, HEALPix pixels are not spherical quadrilaterals because their edges are not great circle arcs.

HEALPix was originally described purely with reference to the sphere, the data itself being stored as a one-dimensional array in a FITS binary table (Cotton et al. 1995) with either *ring* or *nested* organization, the former being suited for spherical harmonic analysis and the latter for nearest-neighbour searches. For visualisation purposes the software that implements HEALPix offers a choice of four conventional projection types onto which HEALPix data may be regridded.

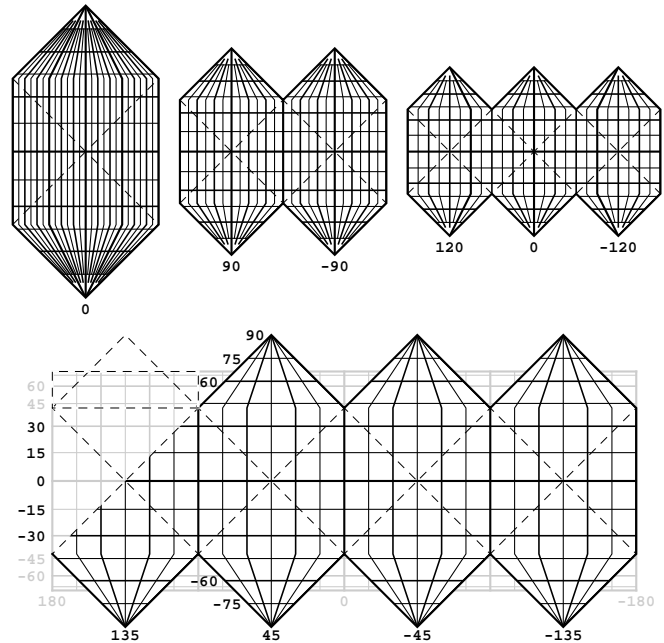


**Fig. 1.** The HEALPix class of projections for  $H = 1, 2, 3$  (top), and the nominative case with  $H = 4$  (bottom) at twice the linear scale and with the top left-hand corner of the graticule “cut away” to reveal the underlying cylindrical equal-area projection in the equatorial region. Facets are shown as dashed diamonds.

However the existence of the analytical mapping of each of the twelve base-resolution pixels onto a  $[0, 1] \times [0, 1]$  unit square was noted, and in fact the HEALPix software uses this. Roukema & Lew (2004) have recently provided a mathematical derivation of the equations and present a diagram showing a projection of the whole sphere (hereinafter the *HEALPix pro-*

Send offprint requests to: M. Calabretta,  
e-mail: mcalabre@atnf.csiro.au

jection) in which the base-resolution pixels, and consequently the pixels of all higher-order pixelisations, are projected as diamonds (i.e. squares rotated by  $45^\circ$ ). These equations may readily be synthesised into those of an equal area projection of the whole sphere.

The HEALPix projection does not appear to have been documented previously in cartography texts and could not be located in a web search; in particular, it is absent from Snyder's (1993) review of the history of cartography, and also from Pearson (1990). Illinois State University's MicroCAM website presents a catalogue of 320 map projections produced by a member of the International Cartographic Association's Commission on Map Projections (Anderson, 2003). None bear even a superficial resemblance; the equal-area quad-cube may be dissected and rearranged to produce something with a similar boundary but it is a distinctly different projection. The stated intention of this website is to present as complete a collection as possible of historical, published map projections.

This work will show that the HEALPix projection is one of the more important members of an infinite class of projections parameterised by  $H \in \mathbb{N}$  and will derive the projection equations for the class. In particular, the HEALPix projection (i.e. with  $H = 4$ ) suggests a simple way of storing HEALPix data on a two-dimensional square grid as used in conventional imaging and mapping, and also suggests an extension of the HEALPix pixelisation that is better suited to this. The HEALPix projections with  $H = 3$ , and 6 are also shown to be special, and their properties will be discussed.

The related issues of representing celestial coordinates in the HEALPix projection are also considered in relation to image data storage in FITS (Hanisch et al. 2001).

## 2. The HEALPix projections

Firstly in this section we derive the projection equations for the infinite class of HEALPix projections. This leads naturally to the subject of mapping HEALPix data on a regular grid and extensions of the HEALPix pixelisation that arise.

### 2.1. HEALPix derivation

Figure 1 shows the first four members ( $H = 1, \dots, 4$ ) of the HEALPix projections. They may be described as interrupted, equal area, pseudo-cylindrical projections whose defining characteristics are

1. They are equi-areal; regions with equal areas on the sphere have equal areas in the plane of projection.
2. Parallels of latitude are projected as horizontal straight lines (interrupted in the polar regions) whence  $\partial y / \partial \phi = 0$ .
3. Parallels are uniformly divided (apart from interruptions).
4. The interruptions are defined by stacking equal-area diamonds (hereinafter *facets*) as shown in Fig. 1. The facet that straddles  $\pm 180^\circ$  is split into halves in the graticule.

#### 2.1.1. Transition latitude, $\theta_x$

In deriving the projection equations, note firstly that for any  $H$  the total area occupied by the half-facets in the north polar region is always  $1/6$  of the total area. Since the projections are equi-areal, we equate the area of a spherical cap on the unit sphere,  $A = 2\pi(1 - \sin \theta)$ , with the corresponding fraction of the total area,  $4\pi/6$ , to obtain the transition latitude,  $\theta_x$ , which is independent of  $H$ :

$$\theta_x = \sin^{-1}(2/3) \approx 41^\circ 8' 10.3. \quad (1)$$

#### 2.1.2. Equatorial region

The equatorial region, where  $|\theta| \leq \theta_x$ , is clearly a cylindrical equal-area projection, i.e.  $(x, y) = (\phi, \alpha \sin \theta)$ , where  $\alpha$  is a constant determined by the requirement that  $\theta_x$  be projected at the vertex of a square, i.e.  $y_x = \pi/H = \alpha \sin \theta_x$ , whence

$$x = \phi, \quad (2)$$

$$y = \frac{3\pi}{2H} \sin \theta. \quad (3)$$

Because  $\partial y / \partial \phi = 0$  for the HEALPix projections the Jacobian reduces to

$$J(\phi, \theta) = \frac{1}{\cos \theta} \frac{\partial x}{\partial \phi} \frac{\partial y}{\partial \theta}. \quad (4)$$

This gives the ratio of an infinitesimal area in the plane of projection to the corresponding area on the sphere. In the equatorial regions it is  $3\pi/2H$ , a constant, indicative of an equi-areal projection. Note that the Jacobian is inversely proportional to  $H$ , but the graticules in the top part of Fig. 1 were set to the same areal scale by scaling  $x$  and  $y$  by  $\sqrt{H}$ .

#### 2.1.3. Polar regions

In the polar regions the area north of  $\theta (> \theta_x)$  on the unit sphere is  $2\pi(1 - \sin \theta)$  and, noting that the pole is projected at  $y = 2\pi/H$ , in the plane of projection it is  $H(2\pi/H - y)^2$ . Equating the ratio of these to the value of the Jacobian obtained for the equatorial region and solving we obtain

$$y = \pm \frac{\pi}{H}(2 - \sigma), \quad (5)$$

where the negative sign is taken for the south polar region, and

$$\sigma = \sqrt{3(1 - |\sin \theta|)} \quad (6)$$

is the ratio of the distance of the pole from the parallel of  $\theta$  to that of the pole from the parallel of  $\theta_x$ .

The equation for  $x$  may be obtained readily by integrating Eq. (4) with  $\partial y / \partial \theta$  from Eqs. (5) & (6) to produce  $x = \sigma \phi + C$ , where  $C$  is the constant of integration, thus indicating that the parallels are uniformly divided. It is instructive also to consider a geometrical argument; the area of any triangle in the  $(x, y)$  plane with its apex at the pole and base along a given parallel of latitude depends only on the change in  $x$  between its base vertices and not on their location. Since the projection is equi-areal,  $x$  must therefore vary linearly with  $\phi$ .

Applying the interruptions to the parallels (which in fact could be omitted or done in other ways to produce different projection types) we have

$$x = \phi_c + (\phi - \phi_c) \sigma, \quad (7)$$

where

$$\phi_c = \frac{\pi}{H} \left( 2 \left\lfloor \frac{(\phi + \pi)H}{2\pi} \right\rfloor + 1 \right) - \pi \quad (8)$$

is the native longitude in the middle of a polar facet and  $\lfloor u \rfloor$ , the *floor* function, gives the largest integer  $\leq u$ .

#### 2.1.4. Properties

The most important feature of the HEALPix projections, indeed the underlying rationale for the HEALPix pixelisation, is that they are equi-areal with squared boundaries. Thus they may be completely inscribed by diamonds of equal area, the minimum number of which is  $3H$  (the facets). Each facet is subject to further subdivision by  $N^2$  smaller equal-sized diamonds that are identified as *pixels*; their centre positions in  $(\phi, \theta)$  may be computed readily for any  $(H, N)$  from the inverse of the above projection equations as are cited in Sect. 2.4. As explained by Górski et al. (2004), it is significant for spherical harmonic analysis that the pixel centres lie on a relatively small number of parallels of latitude, and that the facets may be subdivided in a hierarchical way.

Of course a pixelisation may be constructed similarly from a cylindrical equal-area projection, but the HEALPix projections are much less distorted in the polar regions than any such projection. Consequently the HEALPix pixels are much truer in shape when projected onto the sphere and their centres are much more uniformly distributed. As shown by the dashed lines in the upper-left corner of Fig. 1, the equivalent portion of the underlying cylindrical projection, being severely squashed at the pole, is stretched upwards to twice its height and brought to a point; the pole itself is thereby projected as  $H$  points rather than a line. However, this is gained at the cost of introducing  $H - 1$  interruptions which should properly be considered as extreme distortions, though of little consequence for the pixelisation.

Evaluating the partial derivatives we find

$$\left( \frac{\partial x}{\partial \phi}, \frac{\partial y}{\partial \theta} \right) = \left( 1, \frac{3\pi}{2H} \cos \theta \right) \quad \dots \text{equatorial} \quad (9)$$

$$\left( \frac{\partial x}{\partial \phi}, \frac{\partial y}{\partial \theta} \right) = \left( \sigma, \frac{3\pi}{2H} \frac{\cos \theta}{\sigma} \right) \quad \dots \text{polar} \quad (10)$$

which shows that in the polar regions  $x$  is scaled directly, and  $y$  is scaled inversely by  $\sigma(\theta)$  in order for the Jacobian to maintain constancy.

To get some idea of the relative degree of distortion between members of the class, consider first from Eqs. (3) & (5) that  $y$  scales as  $1/H$  for any  $\theta$ , while  $x$  is independent of  $H$  except for defining the interruptions. Hence the relative spacing of parallels between the equator and poles is independent of  $H$ , as is evident in Fig. 1, and the distortion is determined solely by the relative  $y : x$  scaling.

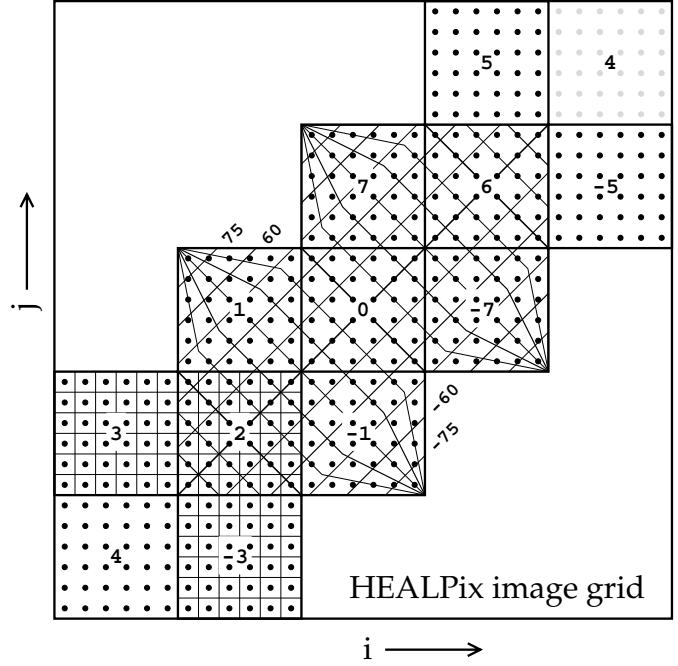


**Fig. 2.** The HEALPix pixelisation for  $N = 6$  on the HEALPix projection for  $H = 4$  projected with a  $45^\circ$  rotation onto the mapping grid showing the twelve facets with a convenient numbering scheme. The graticule of the HEALPix projection is shown in the seven facets adjacent to  $(\phi, \theta) = (0, 0)$ , and those at lower left show the pixel boundaries for  $N = 6$  as defined by the HEALPix pixelisation.

A spherical projection is *conformal* or *orthomorphic* (true shape) at points where the meridians and parallels are orthogonal and equi-scaled. The general equations of the cylindrical equal area projection expressed in terms of the conformal or *standard* latitude,  $\theta_o$ , are  $(x, y) = (\phi, \sin \theta / \cos^2 \theta_o)$  (e.g. see Sect. 5.2.2 of Calabretta & Greisen 2002), whence from Eq. (3)

$$\theta_o = \cos^{-1} \sqrt{\frac{2H}{3\pi}}. \quad (11)$$

For  $H = 1, 2, 3, 4$  this is  $(62^\circ 57', 49^\circ 35', 37^\circ 07', 22^\circ 88')$ ; the first two of these exceed  $\theta_x$  and hence are inadmissible, and  $\theta_o$  is undefined for higher values of  $H$ . Since the latitude that halves the area of the equatorial region is  $\sin^{-1}(1/3) = 19^\circ 47'$ , independent of  $H$ , this suggests that the projection with  $H = 4$  is the least distorted in the equatorial regions.

Looking at it another way, the requirement for equiscaling in  $x$  and  $y$  where the meridians and parallels are orthogonal, i.e. everywhere in the equatorial region, and along the centreline in the polar half-facets, is

$$\frac{1}{\cos \theta} \frac{\partial x}{\partial \phi} = \frac{\partial y}{\partial \theta}. \quad (12)$$

Substituting Eqs. (9) and (10) gives

$$H_o = \frac{3\pi}{2} \cos^2 \theta \quad \dots \text{equatorial} \quad (13)$$

$$H_o = \frac{\pi}{2} (1 + |\sin \theta|) \quad \dots \text{polar, centreline} \quad (14)$$

which gives  $H_o = (4.7, 4.4, 3.5, 2.6, 2.7, 2.9, 3.1, 3.1)$  for  $\theta = (0, 15, 30, \theta_x, 45, 60, 75, 90)$ . Thus  $H = 4$  is a good all-over

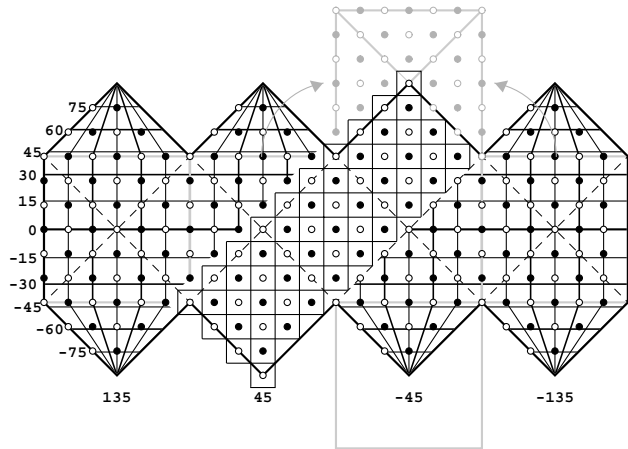


**Fig. 3.** HEALPix double-pixelisation for  $N = 3$  on the HEALPix projection with  $H = 4$ . Filled circles define the regular grid, with interpolated pixels shown as open circles to the *left* of these. Pixel boundaries are shown in the middle three facets, those of the two additional polar pixels contain a contribution from each of the four adjacent polar facets. Note the difference between the pixel locations in this figure compared to the  $N = 6$  pixelisation in Fig. 2. Also illustrated is the boundary between the faces of the pseudo-quadcube layout of the HEALPix projection (grey).

compromise but for  $|\theta| > 30^\circ$ , the latitude that halves the area of the hemisphere,  $H = 3$  would appear to be better on this basis.

The nature of the projective distortion in the region where meridians and parallels are not orthogonal is more complicated. In the polar regions the projection of the facets onto the sphere (i.e. the base-resolution pixels) meet at the pole at  $360^\circ/H$ . For  $H = 4$  this is  $90^\circ$  which accords with the angle in the plane of all HEALPix projections. Thus it might seem that  $H = 4$  should be least distorted in the neighbourhood of the pole. However, this argument is specious; on the sphere the angle between meridians and parallels along the edges of the polar half-facets is always  $90^\circ$ , while in the plane of projection it is always  $45^\circ$ .

These comments on distortion will be qualified in Sect. 2.3 for members of the class for which additional  $y$ -scaling is applied.

## 2.2. The HEALPix grid

The base-resolution pixels of the HEALPix pixelisation are projected as diamonds (squares rotated by  $45^\circ$ ) on the HEALPix projection with the consequence that the pixel locations fall on a grid with diamond-symmetry.

However, Fig. 2 shows that the diamond grid may be converted to the common square grid used in imaging via a trivial  $45^\circ$  rotation. The resulting image plane is slightly less than half-filled (48%) but this is comparable to the figure of 50% for quad-cube projections (O’Neill & Laubscher 1976) which are commonly used in the same type of application as HEALPix. Moreover, being composed of square facets like the quad-cubes, the HEALPix projection also admits the possibility of dissection and storage on a third image axis, such as is imple-

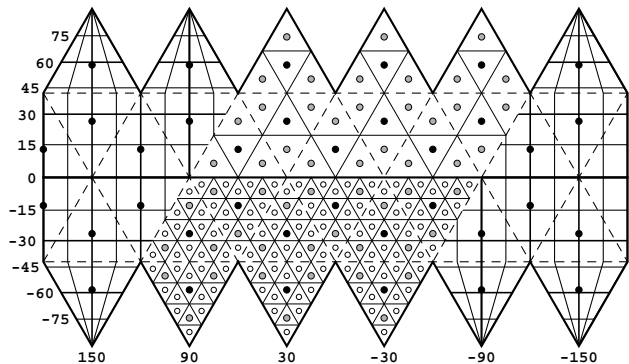


**Fig. 4.** HEALPix projection for  $H = 6$  scaled in  $y$  by  $\sqrt{3}$  whereby the square facets become pairs of equilateral triangles. These may then be subdivided in a hierarchical way; base-level pixels are shown to the left and right (black circles), the first level of subdivision is at mid-top (grey circles), the next at mid-bottom (open circles).

mented for the quad-cubes via the CUBEFACE keyword in FITS (Calabretta & Greisen (2002)). In this context Fig. 3 shows how the facets may be repartitioned into a configuration that resembles that of the quad-cube faces. However, this resemblance is purely superficial because the “cubeface” edges do not match those of a quad-cube projection on the sphere.

Facet number 4 which straddles  $\phi = \pm 180^\circ$  may be treated in a number of ways; it may be left split, or the halves may be reconnected in either the lower-left or upper-right corner, or it may be replicated in both.

### 2.2.1. HEALPix double-pixelisation

The main drawback with the above technique for storing HEALPix imaging data is that the image is presented at an unusual orientation. However, this may be solved via a simple extension to the HEALPix pixelisation. Figure 3 shows the HEALPix grid with a pixel interposed between every pair of pixels along the parallels of latitude and additional pixels added at the two poles. The total number of pixels in the pixelisation is thereby increased from  $12N^2$  to  $24N^2 + 2$  without affecting the special properties described by Górski et al. (2004), although requiring a slightly different method of forming the hierarchy and indexing it. Pixels that fall along the lines where the polar half-facets meet are distorted in such a way as to “zip” the two edges together but they still have equal area.

## 2.3. Other pixelisations

Consider dividing the  $360^\circ$  of circumpolar latitude into integral subdivisions. Of the possible ways of doing this ( $1 \times 360^\circ$ ,  $2 \times 180^\circ$ ,  $3 \times 120^\circ$ ,  $4 \times 90^\circ$ ,  $5 \times 72^\circ$ ,  $6 \times 60^\circ$ , ...) only the divisions into 3, 4, and 6 correspond to regular polyhedra. The division into  $4 \times 90^\circ$  corresponds to the familiar case of HEALPix with  $H = 4$  with diamonds tessellated by diamonds.

### 2.3.1. Triangular – $H = 6$

However, the division into  $6 \times 60^\circ$  suggests a different type of pixelisation in which equilateral triangles are tessellated

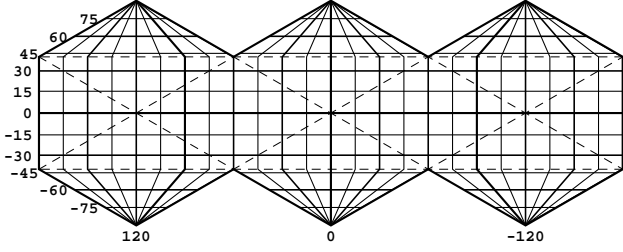


**Fig. 5.** HEALPix projection for  $H = 3$  scaled in  $y$  by  $1/\sqrt{3}$  whereupon it becomes three consecutive hexagons.

by equilateral triangles. This pixelisation may be defined by rescaling the HEALPix projection with  $H = 6$  by  $\sqrt{3}$  in  $y$  so that the half-facets become equilateral triangles. Such a linear scaling does not affect the projection’s equal area property. What were previously half-facets may now be identified with 36 new, triangular base-resolution pixels that may be subdivided in a hierarchical way as for HEALPix, as depicted in Fig. 4. It is interesting to note that this subdivision is naturally hierarchical - the number of pixels varies exponentially as  $36 \times 4^{N-1}$  where  $N$  is the hierarchy level. In the  $H = 4$  pixelisation the exponential hierarchy must be engineered by doubling  $N$ .

The conformal latitude computed for  $H = 6$  with this extra  $y$ -scaling is  $\theta_o = 30^\circ 98'$ , indicating that the projection becomes conformal at the latitude that bisects the hemisphere by area. Applying Eqs. (13) and (14) with the extra scaling gives  $\sqrt{3}H_o = (8.2, 7.6, 6.1, 4.5, 4.6, 5.1, 5.3, 5.4)$  for  $\theta = (0, 15, 30, \theta_x, 45, 60, 75, 90)$ , again indicating less distortion in the polar regions than  $H = 4$ . It also does better in the polar zone away from the centreline because the  $60^\circ$  angle along the edge of the polar facets more closely matches the true angle of  $90^\circ$  on the sphere. Overall, this pixelisation performs adequately at low latitudes and does better than the  $H = 4$  pixelisations at mid to high latitudes.

This rescaling of the  $H = 6$  projection is reminiscent of Tegmark’s (1996) icosahedral projection composed of 20 equilateral triangles; the problem of indexing the subdivisions of its triangular facets was solved in the implementation of the corresponding pixelisation. In the present context the iso-latitude property is still present but modified somewhat from the diamond pixelisation of  $H = 4$ . However, if the pixel centres are moved up or down from the centroid by  $\frac{1}{12}$  of the height of the equilateral triangles to the point half-way between the base and apex then they fall onto a regular grid sampled more frequently in  $x$  than  $y$ . This provides some of the same benefits as the  $H = 4$  double-pixelisation.

However, although the displacement is small, there is a possibility that it will introduce statistical biases so the full consequences should be investigated for a particular application. These potential biases may be minimised by making the pixel size sufficiently small, and the fact that the bias between adjacent pairs of pixels is in opposite senses will tend to cancel them over a region encompassing a sufficient number of pixels. It should also be remembered that although the pixel locations appear to be at the centre of the pixel boundary in the projection of the diamond, square, and triangular pixelisations this

is very much an artifact of the distortions inherent in the projection. Because the  $y$ -coordinate varies non-linearly with  $\theta$ , on the sphere they are actually biased to one side of the pixel. Hence some degree of bias is unavoidable.

### 2.3.2. Hexagonal – $H = 3$

The division into  $3 \times 120^\circ$  suggests hexagonal base-resolution pixels. Although the familiar “honeycomb” structure shows that it is possible to tile the plane with hexagons, nevertheless there is no bounded tessellation of hexagons by hexagons. That is, a hexagonal region may not be cut out of a honeycomb tessellation without cutting the individual elements. Thus it may seem surprising that a hexagonal pixelisation can be constructed from the HEALPix projection for  $H = 3$  with  $y$  scaled by  $1/\sqrt{3}$ . The boundary of this projection, as seen in Fig. 5, is reduced to that of three sequential hexagons. This boundary is then used conceptually as a “pie-cutter” on a honeycomb tessellation of the right scale. Pixels that are cut can be made whole again by borrowing from adjacent facets, much as the square pixelisation in Fig. 3 does.

Rescaling Eqs. (13) and (14) gives  $H_o/\sqrt{3} = (2.7, 2.5, 2.0, 1.5, 1.5, 1.7, 1.8, 1.8)$  for  $\theta = (0, 15, 30, \theta_x, 45, 60, 75, 90)$ . Thus the rescaled  $H = 3$  projection does not achieve conformality at any latitude, it does well close to the equator, but degrades at mid-latitudes. In the polar regions the  $30^\circ$  angle between meridians and parallels along the edge of the facets is further from the ideal of  $90^\circ$  than the  $45^\circ$  for the unscaled projections.

### 2.4. HPX: HEALPix in FITS

In this section the HEALPix projections are described in the same terms as the projections defined in Calabretta & Greisen (2002).

HEALPix projections will be denoted in FITS with algorithm code HPX in the CTYPE*ia* keywords for the celestial axes. As data storage has become much less of an issue in recent years we do not consider it necessary to create an analogue of the CUBEFACE keyword to cover HPX. However, if HEALPix data is repackaged into the pseudo-quadcube layout shown in Fig. 3 the CUBEFACE storage mechanism is applicable for  $H = 4$  and will be treated properly by wcsLIB (Calabretta, 1995).

Since the HEALPix projections are constructed with the origin of the native coordinate system at the reference point, we set

$$(\phi_0, \theta_0)_{\text{HEALPix}} = (0, 0). \quad (15)$$

The projection equations and their inverses, re-expressed in the form required by FITS, are now summarised formally.

In the equatorial zone where  $|\sin \theta| \leq 2/3$ :

$$x = \phi, \quad (16)$$

$$y = \frac{270^\circ}{H} \sin \theta, \quad (17)$$

in the polar zones, where  $|\sin \theta| > 2/3$ :

$$x = \phi_c + (\phi - \phi_c) \sigma, \quad (18)$$

$$y = \pm \frac{180^\circ}{H}(2 - \sigma), \quad (19)$$

where the positive sign on  $y$  is taken for  $\theta > 0$ , negative otherwise, and

$$\sigma = \sqrt{3(1 - |\sin \theta|)}, \quad (20)$$

$$\phi_c = \frac{180^\circ}{H} \left( 2 \left\lfloor \frac{(\phi + 180^\circ)H}{360^\circ} \right\rfloor + 1 \right) - 180^\circ. \quad (21)$$

These equations are readily invertible. In the equatorial zone where  $|y| \leq 180^\circ/H$ :

$$\phi = x, \quad (22)$$

$$\theta = \sin^{-1} \left( \frac{yH}{270^\circ} \right), \quad (23)$$

in the polar zones, where  $|y| > 180^\circ/H$ :

$$\phi = x_c + (x - x_c)/\sigma, \quad (24)$$

$$\theta = \pm \sin^{-1} \left( 1 - \frac{\sigma^2}{3} \right), \quad (25)$$

where the positive sign on  $\theta$  is taken for  $y > 0$ , negative otherwise, and

$$\sigma = 2 - \frac{|yH|}{180^\circ}, \quad (26)$$

$$x_c = \frac{180^\circ}{H} \left( 2 \left\lfloor \frac{(x + 180^\circ)H}{360^\circ} \right\rfloor + 1 \right) - 180^\circ. \quad (27)$$

where  $x_c$  is the value of  $x$  in the middle of a polar facet, as for  $\phi_c$ .

FITS keyword `PVi_1a` attached to *latitude* coordinate  $i$  will be used to specify  $H$  with default value 4.

HPX has been implemented in version 3.7 of `wcslib` which is distributed under a GNU Library Public License (GLPL).

*Acknowledgements.* The Australia Telescope is funded by the Commonwealth of Australia for operation as a National Facility managed by CSIRO.

## References

- Anderson, P. B. 2003, MicroCAM (Computer Aided Mapping) web site (last updated 2003/Aug) [http://www.ilstu.edu/~microcam/map\\_projections/](http://www.ilstu.edu/~microcam/map_projections/)
- Calabretta, M. R. 1995-2004, `wcslib`, version 3.7, available from <ftp://ftp.atnf.csiro.au/pub/software/wcslib/wcslib.tar.gz>
- Calabretta, M. R., & Greisen, E. W. 2002, *A&A*, 395, 1075
- Cotton, W. D., Tody, D., & Pence, W. D. 1995, *A&AS*, 113, 159
- Górski, K. M., Hivon, E., Banday, A.J., Wandelt, B.D., Hansen, F.K., Reinecke, M., & Bartelman, M. 2004, *ApJ* (accepted), arXiv:astro-ph/0409513
- Hanisch, R. J., Farris, A., Greisen, E. W., et al. 2001, *A&A*, 376, 359
- O'Neill, E. M., & Laubscher, R. E. 1976, Extended Studies of the Quadrilateralized Spherical Cube Earth Data Base, NEPRF Technical Report 3 - 76 (CSC) Computer Sciences Corporation (Silver Springs, Maryland)
- Pearson, F. 1990, *Map Projections - theory and applications* (CRC Press, Boca Raton)
- Roukema, B.F., & Lew, B. 2004, arXiv:astro-ph/0409533
- Snyder, J. P. 1993, *Flattening the Earth* (University of Chicago Press, Chicago and London)
- Tegmark, M. 1996, *ApJ*, 470, L81